THE AMERICAN SOCIETY OF MECHANICAL ENGINEERS
345 E. 47th St., New York, N.Y. 10017

96-GT-401

Periodic Aerodynamic Response of Axial Fan Rotor Blades to Nonuniform Inlet Flow Fields

M. Staiger and H. Stetter

Institut für Thermische Strömungsmaschinen und Maschinenlaboratorium
Universität Stuttgart
Stuttgart, Germany

Abstract

An experimental investigation of the aerodynamic response of the rotor blading of a single stage low speed axial research compressor, which was exposed to wake type inlet flow disturbances was carried out at the Institute's low speed compressor and fan research facility. The investigation comprised 5 hole pressure probe surveys of the nonuniform flow field at the rotor inlet and exit planes as well as direct recording of the unsteady surface pressure response by rotor blade mounted 'fast response' miniature pressure transducers. Forcing functions in terms of streamwise and transverse gust velocities were determined from the circumferential and radial distribution of the inlet flow properties. The blade surface pressure history of the unsteady aerodynamic response was recorded at several locations along span and along chord. The influence of steady stage loading on the forcing function as well as on the unsteady rotor blade response was investigated. At midspan the recorded local blade surface pressure histories were integrated to a spanwise unsteady blade force coefficient, which was correlated to a calculated force coefficient determined by a twodimensional linearized unsteady aerodynamic analysis.

Introduction

In quite a few instances excessive dynamic blade stresses are to be blamed for blade failure in turbomachines of all kinds. Especially the first stages of gas turbine engines or industrial axial flow compressors as well as the rotor blades of modern high performance axial draft fans for the power and mining industry, which are quite often subject to wake type inlet flow disturbances, may suffer from a high level of cyclic blade bending and blade torsional stresses. This is due to the fact, that the moving rotor blade experiences the low energy wakes of the inlet flow field, which are stationary with respect to the machine's housing, as periodic changes in aerodynamic loading. The resulting engine order forcing may generate serious blade vibration amplitudes especially in the case of resonance, when a blade forcing frequency coincides with one of the blading's natural frequencies, and when in addition the forcing pattern matches the deflection pattern of that particular blade mode.

In order to prevent blade failure due to high cycle fatigue, the level of the periodic blade stresses during operation as well as potential resonance hazards should already be known quite accurately during the design procedure. An accurate preevaluation of the dynamic rotor blade stresses requires the knowledge of the blading's natural vibration behaviour, the knowledge of the intensity and frequency of blade forcing and of the damping. At the present state a good base of knowledge and experience is available in the field of modelling the natural vibration behaviour of axial turbomachinery blading. Whereas the field of quantifying the unsteady aerodynamic blade response associated with the aerodynamic interaction of upstream wake flows with a moving turbomachinery blade row is still an area of intense research and CFD code development. Since the first introduction of solutions to the unsteady rotor blade loading problem in turbomachines [1,2] tremendous progress in modelling unsteady blade loading has been made. The development in calculation codes up to the 1990s is summarized in [3,4]. The ability of current engineering/analysis models to predict unsteady aerodynamic loading of gas turbine blades is comprehensively discussed in [4]. Thereby the stator blade surface pressure response to rotor blade wakes, which were predicted by various calculation codes, is compared to experimental data obtained in a low speed research compressor. A complete blade forced response analysis system as well as the results of a simulation of a fan blade forced response to large scale inlet flow disturbances were introduced in [5]. Thanks to the recent development in modern data sampling techniques, based on micro sensors, which allow recording of unsteady flow properties inbetween blade rows and/or on moving blade surfaces, a growing number of data sets, obtained in real compressor environments, became available for code validation since the mid 1980s.

An important issue in wake induced blade response analysis is the prediction of the wake strength, which influences the forcing function. In [6,7] detailed investigations of wake flows downstream of typical compressor components such as inlet guide vanes, stator blades and rotor blades are presented. Based on the similarity of velocity profiles across the wake flow a mathematical relation to

Presented at the International Gas Turbine and Aeroengine Congress & Exhibition
Birmingham, UK — June 10-13, 1996

model the change in wake flow characteristics with growing distance to the wake causing body, e.a. the growth in wake width and the attenuation of the velocity defects, is given. These semi empirical relations are validated by near midspan hot wire measurements in a real compressor environment. In [8] the wake profile prediction capabilty of a 3D CFD solver is discussed. The predicted wake shapes are thereby compared to wake velocity profiles measured downstream of compressor rotor blades as well as of turbine rotor blades. Results from direct recordings of forced blade pressure responses, i.e. time histories of unsteady blade surface pressures, are shown in [9-13]. These meaesurements comprised the response of stator blades to an upstream moving rotor row as well as the response of a moving rotor blade row to stationary wake type inlet flow disturbances of different reduced frequencies. The unsteady blade surface pressure associated with the phenomenon of rotor blade flutter was investigated in an axial research compressor stage [14]. Due to the limited space available for instrumentation in compressor blade rows, most of the experimental data were recorded at/near midblade sections, where the flow through the blade channel is usually least affected by threedimensional flow effects such as endwall boundary layer, tip leackage flows, etc.. Furthermore most of the investigations concentrate on the high frequency interference between successive blade rows in a multistage environment or on the interaction with inlet flow distortions, which affect a large portion of the inlet crossectional area.

The investigations reproted in this paper focus on low frequency blade forcing due to wakes of struts, which are typically found in the annular inlet flow channel of stationary machines. Such support struts usually have a substantial thickness compared to the streamlined IGV or stator blades. Therefore they may cause stronger wake defects and subsequently stronger blade forcing. The low frequency forcing associated with only a few struts along the casing circumference is especially dangerous with regard to resonant excitation of lower blade modes, which allow large deflections of the blading. A series of experimental investigations was initiated, intending to identify and to quantify aerodynamic forcing parameters as well as the resulting aerodynamic blade responses due to strut wakes, thereby furnishing a fundamental database, which may help to understand and to model the governing parameters of the unsteady aerodynamic blade/wake interaction.

Test Facility and Instrumentation

Location D/D_a [-]	0.90	0.75	0.60
Blade radius R [mm]	337.5	281.3	225.0
Chord s [mm]	89.3	89.3	89.3
Blade angle λ [deg.]	22.8	29.7	39.8
Solidity	0.50	0.60	0.76
Distance a [mm]	$a_s + 34.6$	$a_s + 31$	$a_s + 27.4$

Number of Rotor Blades : 12
Rotor Tip Diameter : 750 mm
Rotor Blade Airfoil : NACA 63-510 (circular camber line)
Rotor Blade Twist : $R * c_{2,tan} = constant$
Number of Outlet Guide Vanes (OGV) : 11
Shape of OGV : Flat Plate, twisted, circular camber line

Table 1: Geometry of Single Stage Low Speed Research Compressor

The investigations were carried out at the Institute's low speed single stage compressor research facility. This research facility is specifically designed for the examination of unsteady turbomachinery aerodynamics. Therefore it uses typical axial fan blades with a hub to tip ratio of 0.5, which are large enough to provide sufficient room for the 'on blade' instrumentation at different blade radii D/D_a. The low speed compressor rotor is driven by a variable rpm 90 KW DC motor. The test facility is equipped with a segmented butterfly valve and an auxillary fan, responsible for load variation, and a large silencing chamber, which is directly upstream of the test specimen's inlet. Data sampling from the test cell is fully computerized.

Pressure Probe Measurements

The circumferential flow field pattern, which serves as a base for the definition of a periodic aerodynamic forcing function, is recorded by 5 hole pressure probes in two annular planes close to the rotor, defined as the rotor inlet and the rotor exit planes (Figure 1). During the experiments the rotor blading was subject to typical wake type inlet flow disturbances, which are generated by cylindrical struts, mounted into the short annular flow channel following the inlet bellmouth. The upstream struts were mounted in a special rotatable hub cylinder. The circumferential survey of the flow field was achieved by the struts travelling past the pressure probes, which were stationary with respect to the machine's casing. The incremental hub cylinder rotation as well as the spanwise traversing of the probes were actuated by computer controlled stepping motors.

Blade Surface Pressure Measurements

The aerodynamic rotor blade response to a circumferentially inhomogeneous inlet flow field is represented by the periodically fluctuating blade surface pressures. The local rotor blade surface pressures were monitored by means of fast response miniature pressure transducers of type LQ 125-5SG (Kulite). Thanks to their small size (9.7 mm by 3.2 mm by 0.9 mm in overall dimensions) several LQ 125s could be embedded surface bound into one rotor blade. Transducer locations were chosen in chordal as well as in spanwise direction (Figure 3). At certain locations pressure transducers were applied in pairs i.e. to the blade suction side as well as to the blade pressure side. The pressure signals were transmitted from the rotating reference frame to the stationary environment via radio telemetry. The signals were recorded on a magnetic tape recorder for further processing. A 'one per revolution' trigger signal ensures the correct ensemble averaging procedure of the signals.

The blade mounted pressure transducers were statically calibrated in a temperature controlled chamber. The transducer accuracy is better than ± 1.00 % determined by a least square fit. The nominal natural frequency of the LQ 125 transducer is 70 kHz. This is well above the frequency range of interest (0 to 1.5 kHz). Since the transducers were mounted surface bound, their response performance is not affected by a cavity or a short channel ahead of the membrane. Blade vibrations, however, may seriously bias the pressure signals of blade mounted transducers. This is basically due to the transducer membrane experiencing accelarations acting perpendicular to it, as well as the transducer housing undergoing cyclic straining. The second effect may be minimized by using a certain attachement technique, where the transducer is not attached to the blade surface through a rigid interface. Following suggestions, gi-

ven in [15], the transducers were bonded onto carrier shims, which rigidly adhere to the blade surface at only one end with the other end floating in permanently elastic silicone (RTV) rubber (Figure 3). Thus blade strains were not transfered to the transducer housing. Prior to the forced response measurements the transducer response to blade vibrations was surveyed with no pressure load applied. Blade excitation was provided by a frequency controlled electrodynamic shaker. This vibration test showed, that the blade vibratory response is not strong enough to affect the transducer reading significantly, as long as the excitation frequency does not meet a natural frequency of one of the first two blade modes. The procedure was repeated with the complete instrumented rotor, yielding to the same experience. Thereby resonant vibration of the blading was achieved by choosing the appropriate rotor speed in connection with the appropriate strut pattern generating wake induced blade forcing. Strain gauges were used to monitor the vibratory response of the blading [16]. During test runs with surface pressure recording resonant vibration of the blading was avoided, in order to keep transducer signals due to 'non pressure' effects at a negligible level.

Test Program and Reference Quantities

Wake induced aerodynamic forcing throughout the tests was varied by altering the strut configurations and changing the compressor load. The discussion in this paper primarily focuses on test runs, where the compressor stage was operated at optimum efficiency at a rotorspeed of 2100 rpm ($c_{ax}/u_{tip} = 0.335$, Figure 2). The wake generating strut pattern comprised 5 equally spaced, cylindrical struts of equal thickness pointing radially outward (diameter d_s either 22 mm or 33 mm). At all test runs (except the one, where the parameter a_s/d_s was varied) the struts were located upstream of the rotor blade leading edge at a midspan axial distance a (Figure 1) equal to 55 % of the channel height.

Throughout the paper all flow velocities, which were determined from pressure probe readings, are referenced to the rotor blade tip speed u_{tip}, whereas all pressures and all pressure differences, regardless whether they are determined from pressure probe readings or from signals of the blade mounted transducers, are normalized by the 'artificial' dynamic pressure based on u_{tip}. The quantities normalized in this way may directly be compared to the performance characteristics of the fan stage (Figure 2), thus visualizing the quantitative aspects of the wake flow defects and the wake induced effects at the blade surfaces. Sectional blade forces, determined from the blade pressure response and termed as spanwise blade force coefficients, are referenced to sectional steady state blade forces, evaluated from the aerodynamic performance data of the stage. For convenience in comparing the pressure probe data of the stationary reference frame to the timevariant surface pressure data, recorded in the rotating reference frame, the time axis of the unsteady signals was transformed into the circumferential casing coordinate axis (Figure 1).

Pressure and Velocity Field at Rotor Inlet and Rotor Exit

The angular distribution of flow properties across a single wake region at three different blade radii is presented in Figure 4 and Figure 5. The pressure probe readings clearly show, that strut configurations, which are typical for stationary machines, lead to substantial velocity defects at the rotor inlet. Mainly due to the deficit in axial throughflow velocity the dynamic pressure of the free stream velocity is almost totally lost in the wake region. Furthermore the static pressure falls below its level at the adjacent free stream flow regions, giving rise to flow acceleration and deflection towards the wake center, as can be seen from the increasing tangential flow components in the outer wake regions on either side of the wake center. At the rotor inlet plane the pressure and velocity defects grow continuously from the hub region to the tip region. Due to the static pressure defect profile along span the wake flow field also shows a radial component increasing with radius and deflecting the wake flow towards the upper blade regions. Outside of the wake region there is neither a radial velocity component nor a substantial tangential velocity component of the incoming flow (Figure 5). The pressure probe measurements between rotor and stator blade row show, that the pressure field downstream of the rotor is only very slightly affected by the wake induced flow field disturbance on the rotor suction side. As may be seen from Figure 4, the local total as well as the local static pressure downstream of the rotor do not show any significant circumferential or radial variation. From a comparison of the local pressure fields upstream and downstream of the rotor it may be concluded, that the local unsteady aerodynamic loading of a rotor blade, travelling through the wake region, depends on blade radius.

Wake Characteristics of the Inlet Flow Field

The velocity defect profiles across the wakes of cylindrical struts show the same similarity, as it was observed in the wakes of profiled or streamlined bodies [6,7]. Therefore the experimentally determined midspan wake flow characteristics may also be correlated with the mathematical relation, which was introduced in [6]. It describes the decay of the wake velocity defect and the growth of the wake half width with growing downstream distance to the wake causing obstacle. The results are shown in Figure 6a and 6b, where the ratio of the maximum velocity defect $\Delta_{cax,max}$ in axial throughflow velocity and the development of the wake half width is plotted versus the dimensionless axial distance a_s/d_s. The relation representing the growth of the half width was slightly modified, in order to match the experimental data. The general correlation with the experimental data seems to proof the applicability of the concept given in [6] to model the wake propagation downstream of blunt bodies (cylindrical struts) as well. This concept, however, is restricted to the midblade sections, where the flow is least affected by 3-D effects, as may be seen from Figure 6c, where the maximum wake velocity defect is plotted versus the dimensionless blade radius D/D_s (for a_s/d_s = constant).

Rotor Blade Forcing Function

The periodic unsteady circulation of the flow around the rotor blade and the resulting fluctuations in blade forces originate from the periodic fluctuation of the inlet flow vector w_1 of the rotor based reference system. The time variant relative inlet flow vector w_1 may be obtained by applying the velocity triangles (Figure 7) to each record of the circumferential distribution of the stationary wake velocity vector c_1 (Figure 5). The periodic gust velocity fluctuations parallel (streamwise) and perpendicular (transverse) to the mean relative inlet flow vector w_{1m}, which represents the steady state blade loading (Figure 7), are termed as blade forcing function. For the strut pattern under consideration at an axial distance of $a_s/d_s = 1.56$ ahead of the data sampling plane, the periodic midspan transverse gust velocity reaches values of up to 15% of the blade tip speed u_{tip}. The transverse gust primarily represents the incidence angle fluctuation and has therefore to be looked upon as the crucial forcing function component

governing the unsteady lift. Due to the wake shape along blade span also the gust velocity fluctuations increase from hub to blade tip (Figure 8).

Fourier analyzing the periodic gust velocity distribution yields the engine order forcing functions in terms of the harmonic gust velocity fluctuations $\Delta w_{q,i}$ and $\Delta w_{l,i}$ (Figure 8), which are used as forcing function boundary conditions at classical linearized unsteady aerodynamic analyses. The engine order transverse gust forcing amplitudes exceed the corresponding streamwise gust amplitudes and thereby reach values up to around 3% of u_{tip} at midspan. This value corresponds to about 10% of the average axial throughflow component $c_{ax\infty}$. From the harmonic content it may be seen, that this particular strut arrangement (Figure 1) generates engine order excitations of the order 5 and multiples of 5, where only a slow decrease of the forcing amplitudes with increasing harmonic order of the forcing coefficients is observed. I.e. that engine orders of higher order may have to be taken into account as potential aerodynamic excitation of blade natural modes as well.

Rotor Aerodynamic Response

Figure 9 shows the time history of the unsteady rotor blade surface pressure profiles on the blade pressure side as well as on the blade suction side. All transducer signals were ensemble averaged over at least 64 rotor revolutions and represent the local periodic surface pressure history of one rotor revolution. Figure 10 shows the time history of the corresponding blade surface pressure difference profile. The local pressure difference signals were thereby obtained from a phase controlled superposition of the signals from corresponding suction side and pressure side transducers.

The pressure history plots clearly show, that the flow past the rotor blades is severely influenced by the inlet flow field with its wake type disturbances originating from the struts, located at circumferential coordinates of 0^0, 72^0, 144^0, 216^0 and 288^0 (Figure 1). The magnitude of the unsteady surface pressure fluctuations decays from the leading edge (x/s = 6%) towards the trailing edge of the rotor blade, meaning that the amplitudes from near the leading edge chordal locations contribute most to the unsteady lift force of the particular blade section. Along the blade span the response amplitudes increase with radius. The pressure difference fluctuation amplitudes recorded at a chordal position of x/s = 0.06 double from the lower blade section at $D/D_s = 0.60$ to the upper blade section of $D/D_s = 0.90$, thereby reaching an order of magnitude of about 2.5 times the total pressure rise of the fan stage at optimum efficiency.

A Fourier Analysis of these local unsteady pressure response histories was performed by an ONOSOKKI CF 960 dynamic signal analyzer. Their harmonic content shows, that the rotor response is dominated by the harmonic order of 5 and its higher harmonics as well. In contrast to the forcing function amplitudes the harmonic surface pressure amplitudes decay more rapidly with increasing harmonic order. This is due to the fact, that the unsteady blade response amplitudes are not only a function of the forcing function amplitude but also of the reduced frequency Ω. With increasing unsteadiness, i.e. with growing reduced frequency, the actual unsteady blade response amplitude decreases compared to a theoretical quasi steady ($\Omega = 0$) response amplitude based on the same forcing function amplitude. Based on semichord and the relative inlet flow vector w_{1m} the reduced frequency of the fundamental forcing order due to the strut pattern (5^{th} e.o.) was 0.73.

If the fan stage was loaded at a constant rotor speed from maximum flow rate at $c_{ax}/u_{tip} = 0.37$ to maximum total pressure head at $c_{ax}/u_{tip} = 0.27$ (Figure 2), it was found, that the harmonic surface pressure amplitudes on the blade suction side as well as on the blade pressure side strongly depend on flow rate. This may be seen from Figure 11, where the first four harmonic response amplitudes (due to the forcing strut pattern of 5 equally spaced rods) are plotted versus the dimensionless flow rate c_{ax}/u_{tip}. The response amplitudes shown in Figure 11 were recorded by the transducer pairs at a chordwise position of 6%. The designer may conclude therefrom, that unavoidable wake causing flow obstacles are to be placed into inlet flow areas of lowest possible flow velocity, in order to keep their forcing effects onto the rotor blades at a minimum. In Figure 12 the chordwise distribution of the 5^{th} e.o. surface pressure amplitudes (fundamental order of the forcing strut pattern) is presented. These data are based on experiments downstream of 5 thinner struts (Ø 22mm) and on fan stage operating conditions of maximum flow rate $c_{ax}/u_{tip} = 0.37$. At midspan suction side as well as on midspan pressure side the fundamental surface pressure amplitudes continuously decrease along chord.

Unsteady Blade Forces

When integrating the measured unsteady surface pressure difference profile along the blade chord of a particular blade section, a spanwise unsteady blade force coefficient is obtained. The lower diagram of Figure 13 shows the periodically fluctuating part of the spanwise unsteady blade force, obtained from the pressure readings at midspan. The fluctuating blade force normal to the chord, which may be considered to be approximately equal to the unsteady blade lift force, reaches a value of about 17% of the steady state blade normal force. This value may in reality be larger, since the immediate leading edge region was not considered for the integration due to the lack of pressure transducer information. However the highest pressure fluctuations, being a strong contribution to the unsteady blade forces and moments, have to be expected from that blade region. Therefore the calculated value of the unsteady lift force, using a single airfoil approach [17] may not be as far off the reality, as it seems to be from a first glance onto the two curves shown in the lower diagram of Figure 13. The calculation model is based on the 'Thin Airfoil Theory' and uses the harmonic gust velocity fluctuations (streamwise and transverse) as gust forcing function boundary conditions. The single airfoil approach, however, does not account for the interfering effects of the unsteady circulation of blades adjacent to the blade under consideration and may therefore overpredict the unsteady lift amplitudes. However as far as the phase prediction is concerned, the calculated unsteady blade lift history corresponds reasonably well to the instantaneous forcing incidence fluctuation at the blade leading edge which was derived from the pressure probe data (upper diagram of Figure 13).

When following the rotor blade on its path through the wake region, the flow incidence first decreases due to the corrotating component c_{un} of the wake velocity. When further travelling towards the wake center the instantaneous incidence rapidly increases. Synchronously the time variant blade lift force coefficients first decrease before they sharply increase to their maximum values, which were reached shortly after having passed the wake center. These inci-

dence angle departs Δi of 10^0 and more from the mean incidence i_m means, that the flow around the blades may experience dynamic stall conditions, thereby temporarily generating larger blade lift, as could be expected from the steady state airfoil characteristics [18,19]. The term 'dynamic stall' refers to the unsteady separation phenomena of the airfoil suction surface flow, when an airfoil is oscillating into and out of stall. Dynamic stall thereby begins at an angle of attack larger than the static stall angle, meaning that the blade oscillation and the resulting unsteady flow delay the onset of blade stall. The incidence fluctuation at the leading edge of fixed turbomachinery blades passing wake type inlet flow regions resembles the incidence fluctuations experienced at the leading edge of an airfoil oscillating in pitch. Therefore the unsteady flow around fan blades may be affected in a similar way. In [20] dynamic stall effects at a turbomachinery blade row in conjunction with incidence fluctuations were addressed for the first time. In an experimental investigation dynamic stall phenomena on an instrumented vane row were identified by blade mounted pressure transducers. Recent wind tunnel experiments with 2D single airfoil sections undergoing a cyclic pitching motion showed, that the amount of extra unsteady lift obtained when exceeding the static stall incidence in unsteady motion, depends on a number of variables, with the most important being the rate of change in incidence, the overall deviation from mean steady incidence, the staedy blade loading and the state of the blade suction side boundary layer downstream of the leading edge [19,21]. A quantification of these phenomena associated with 'dynamic stall' on a basis, which could serve for design purpose in turbomachine technology, has not been reported yet.

Recalling the wake shapes, recorded at the three different radii at rotor inlet, it becomes apparent, that the wake width (in circumferential coordinate) does decrease with growing blade radius (Figure 1). The upper rotor blade sections, therefore, pass the wake bome flow field discontinuity within relatively shorter time span, than the lower blade sections do, thereby leading to higher rates of change in incidence at the upper blade sections. According to the observations made at single airfoils oscillating in pitch these higher rates in change of incidence result in higher values of temporary lift forces beyond the static stall limit. This may serve as a qualitative explanation for the fact, that the wake induced, unsteady rotor blade forces increase with blade radius.

Conclusion

Wake type disturbances at inlet flow fields to axial compressor or fan blading have to be considered as serious aerodynamic forcing of the rotor blading. Typical wake borne harmonic gust velocity reach magnitudes of up to 15% of the axial throughflow velocity component of the stationary reference frame, creating lift force fluctuations of the order of magnitude of up to 20% of the steady state blade bending force. In the case of wake type inlet flow field disturbances, equally spaced around the flow channel circumference, the resulting engine order blade forcing is equal to the number of events and its first few higher harmonics. Known mathematical approaches, describing wake characteristics of turbomachinery blade rows and transfering an unsteady inlet flow forcing function into spanwise unsteady blade lift coefficients, may also be used to obtain a first estimate of the magnitude of the unsteady periodic blade forces generated by wake type inlet flow disturbances.

References

[1] Sears, W.R., 1941, *Same Aspects af Nanstatianary Airfail Theory and ist Practical Applicatians.* Journal of Aeronautical Science Vol. 8, pp 104 - 108

[2] Kemp, N.H.; Sears, W.R., 1955, *The Unsteady Forces Due ta Viscous Wakes in Turbamachines.* Journal of Aeronautical Science, Vol. 22, pp 478-483

[3] Hall, K.; Crawley, E., 1987, *Calculation af Unsteady Flows in Turbomachinery Using the Linearized Euler Equations.* Proceedings of the 4th Symposium on Unsteady Aerodynamics and Aeroelasticity of Turbomachines and Propellors, Aachen, Germany

[4] Manwaring, S.R.; Wisler, D.C., 1992, *Unsteady Aerodynamics and Gust Response in Compressars and Turbines.* ASME 92-GT-422

[5] Chiang, H.-W., D.; Kielb, R.E., 1992, *An Analysis System far Blade Forced Respanse.* ASME 92-GT-172

[6] Laksminarayana, B.; Davino, R., 1980, *Mean Velocity and Decay Characteristics af the Guidevane and Statar Blade Wake af an Axial Flow Compressor.* ASME Journal of Engineering for Power, Vol. 102

[7] Laksminarayana, B.; Ravindranath, A., 1980, *Mean Velocity and Decay Characteristics af the Near- and Far - Wake of a Campressor Ratar Blade of Moderate Loading.* ASME Journal of Engineering for Power, Vol. 102

[8] Iszak, M.,S.; Chiang, H.-W.,D., 1993, *Turbine and Campressor Wake Modelling for Blade Forced Response.* ASME 93-GT-236

[9] Manwaring, S.R.; Fleeter, S., 1991, *Farcing Functian Effects an Rator Periodic Aerodynamic Respanse.* ASME Journal of Gasturbines and Power, Vol. 113

[10] Manwaring, S.R.; Fleeter, S., 1990, *Inlet Distartian Generated Periodic Aerodynamic Ratar Response.* ASME Journal of Gasturbines and Power, Vol. 112

[11] Capece, V.R.; Fleeter, S., 1989, *Experimental Investigatian of Multistage Interaction Gust Aerodynamics.* ASME Journal of Gasturbines and Power, Vol. 111

[12] Wallmann, T., 1980, *Experimentelle Untersuchung zur Wechselwirkung zwischen stehenden and umlaufenden Schaufelreihen einer Unterschall - Axialverdichterstufe.* Dissertation, RWTH Aachen

[13] Grollius, H. W., 1980, *Experimentelle Untersuchung von Rotornachlaufdellen und deren Auswirkungen auf die dynamische Belastung axialer Verdichter- und Turbinengitter.* Dissertation, RWTH Aachen, 1980

[14] Hardin, L.W.; Carta, R.O.; Verdon, J.M., 1987, *Unsteady Aerodynamic Measurement on a Compressor Blade Row at Low Ma - Number.* ASME 87 - GT - 221

[15] Grant, H.P.; Lanati, G.A.,1978, *Instrumentation for Measuring the Dynamic Pressure on Rotating Blades.* UTR, N79-12418

[16] Staiger, M.; Zwiener, K.-P.; Stetter, H., 1993, *Effects of Distorted Inlet Flows on Blade Vibrations of Axial Fans.* Proceedings of the IMECHE seminar on 'Installation Effects in Fan Systems', IMECHE, London

[17] Naumann, H.; Yeh, H.,1973, *Lift and Pressure Fluctuations of a Cambered Airfoil under Periodic Gusts and Applications in Turbomachinery.* ASME Journal of Engineering for Power, 1973, (ASME 72 GT 30)

[18] Carta, F.O., 1967, *Usteady Normal Force on an Airfoil in a Periodically Stalled Inlet Flow.* Journal of Aircraft Vol. 4, No. 5

[19] Carr, L.W., 1988, *Progress in Analysis and Predictian of Dynamic Stall.* Journal of Aircraft Vol. 25, No. 1

[20] Henderson, G.H.; Fleeter, S., 1994, *Vortical Gust Response of a Low Solidity Vane Row Including Steady Loading and Dynamic Stall Effects.* ASME 94-GT-295

[21] McCroskey, W.J.; Carr, L.W.; McAlister, K.W., 1976, *Dynamic Stall Experiments on Oscillating Airfoils.* AIAA Journal Vol. 14, No. 1

Nomenclature

a = axial distance to strut (Fig. 1)
c_1 = absolut inlet flow vector
c_2 = absolut flow vector at rotor exit
c_{ax} = axial component of c_1
$c_{ax\infty}$ = mean axial throughflow velocity
Δc_{ax} = local velocity defect
$\Delta c_{ax,max}$ = Δc_{ax} at wake center
C_D = drag coefficient
$Cp = 2 * p / \rho * u_{tip}^2$
Cp_p = dimensionless pressure surface pressure
Cp_s = dimensionless suction surface pressure
$Cp_{p,ith}$ = i^{th} harmonic pressure surface pressure coefficient
$Cp_{s,ith}$ = i^{th} harmonic suction surface pressure coefficient
c_{rad} = radial component of c_1
c_{tan} = circumferential component of c_1
D = local blade diameter
D_a = blade tip diameter
d_s = strut diameter
e.o. = engine order
i_m = mean incidence of w_{1m}
i = incidence w_1 (Fig. 7)
Δi = incidence deviation from i_m
p = blade surface pressure
p_{amb} = ambient pressure
Δp_{tot} = total pressure head of fan stage
R = blade radius
s = chord length
u_{tip} = blade tip speed
w_1 = relative inlet flow vector at blade leading edge
w_{1m} = mean inlet flow vector
Δw_q = transverse gust velocity
Δw_l = streamwise gust velocity
$\Delta w_{q,i}$ = i^{th} harmonic of Δw_q
$\Delta w_{l,i}$ = i^{th} harmonic of Δw_l
x = chordal coordinate
η = efficiency
Ω = reduced frequency
ρ = density
$\Delta\varphi_{HB}$ = wake half width
$\Delta\varphi_{ST}$ = circumf. projection of strut
$\psi_{tot} = 2*\Delta p_{tot} / \rho*u_{tip}^2$ = dimensionless stage pressure bead

Acknowledgement

The work presented was part of two research projects, commissioned by the Forschungsvereinigung für Luft- und Trocknungstechnik (FLT) and the Arbeitsgemeinschaft Industrieller Forschungsvereinigungen (AIF). Both projects (AIF 7462 and AIF 8115) were sponsored by the German Federal Governement (Ministry of Economic Affairs). The author would like to thank for the sponsorship and the assistance.

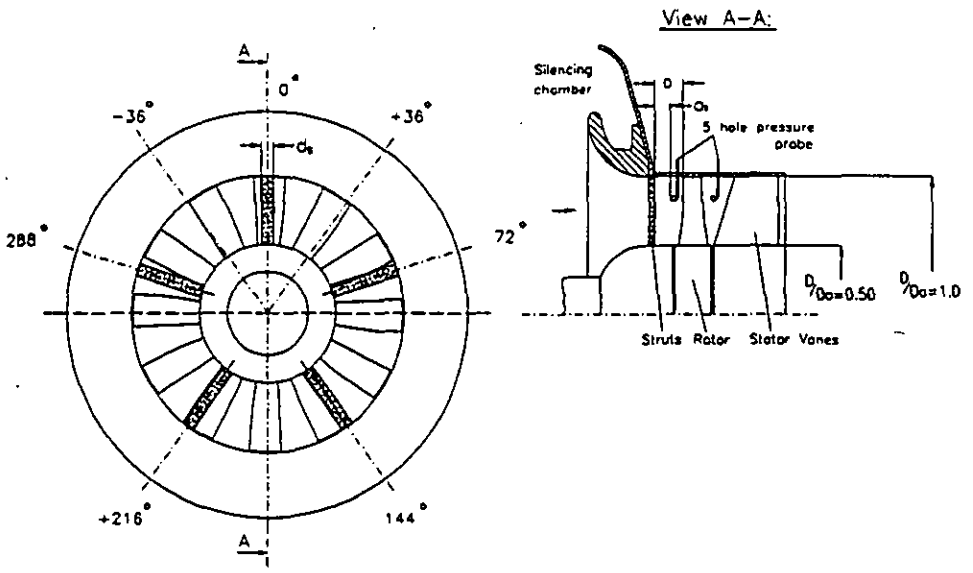

Figure 1 Research fan stage with preessure probe instrumentation

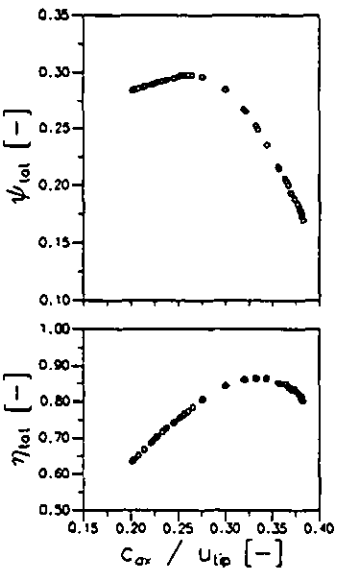

Figure 2 Fan stage performance

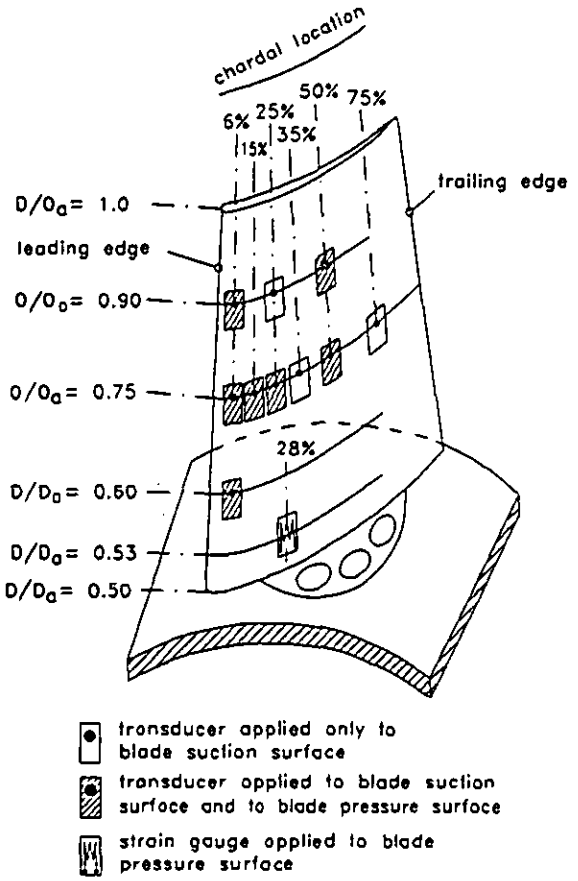

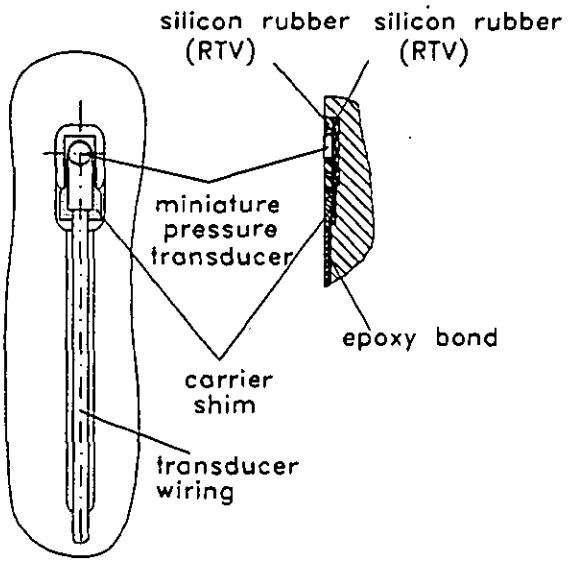

Figure 3 Rotor blade with embedded miniature pressure transducers for unsteady surface pressure recording

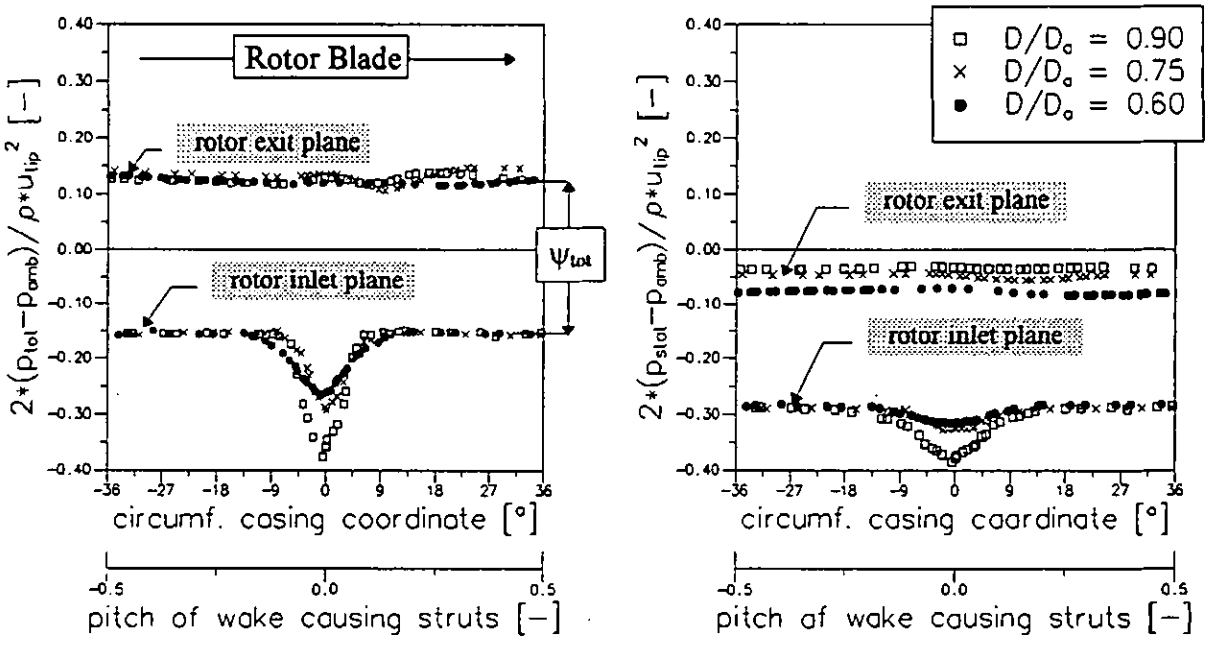

Figure 4 Pressure field upstream and downstream of the fan rotor

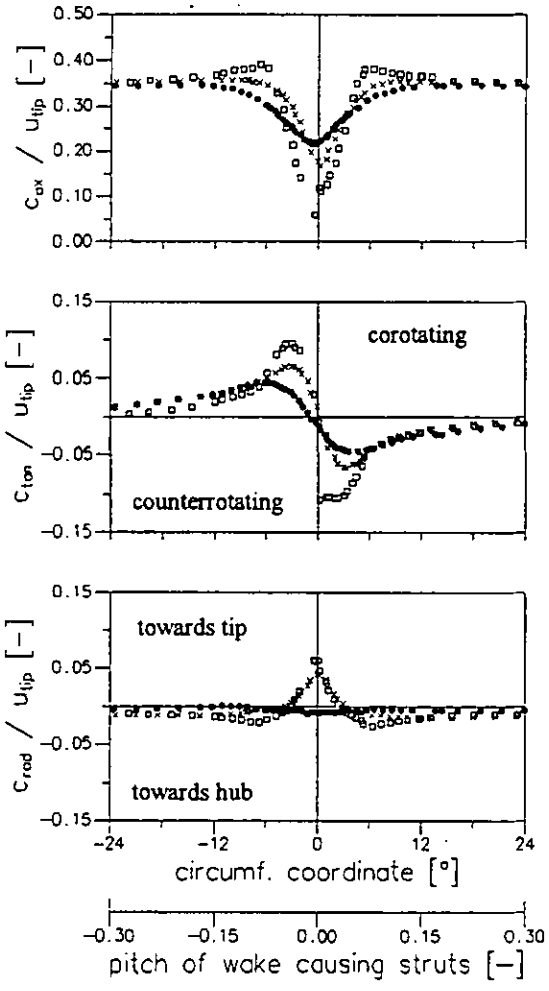

Figure 5 Flow velocity field at rotor inlet plane (absolute flow velocity vector c_1)

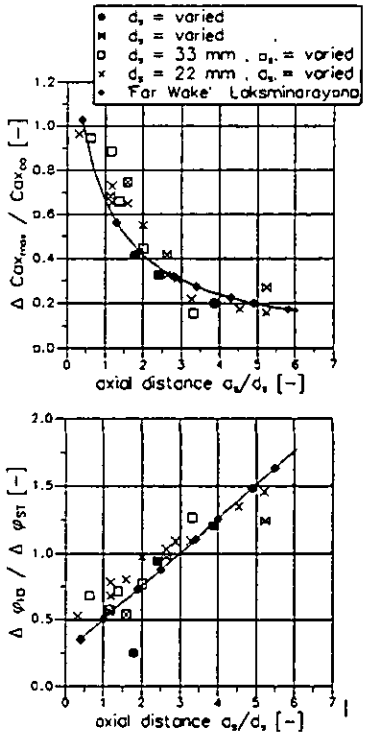

Figure 6a Wake characteristics vs. distance parameter a_s/d_s

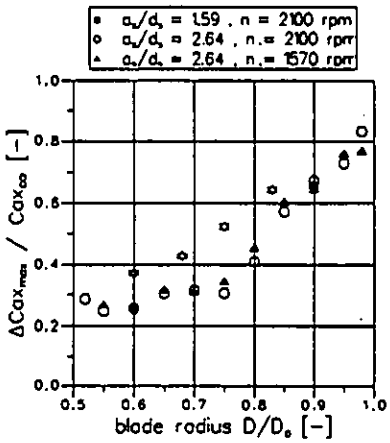

Figure 6b Maximum velocity defect versus blade span D/D_a

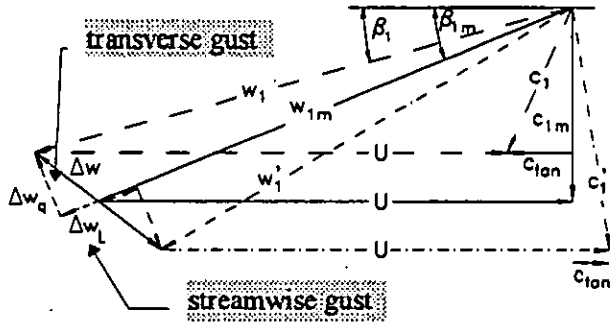

Figure 7 Velocity triangles at the rotor inlet plane

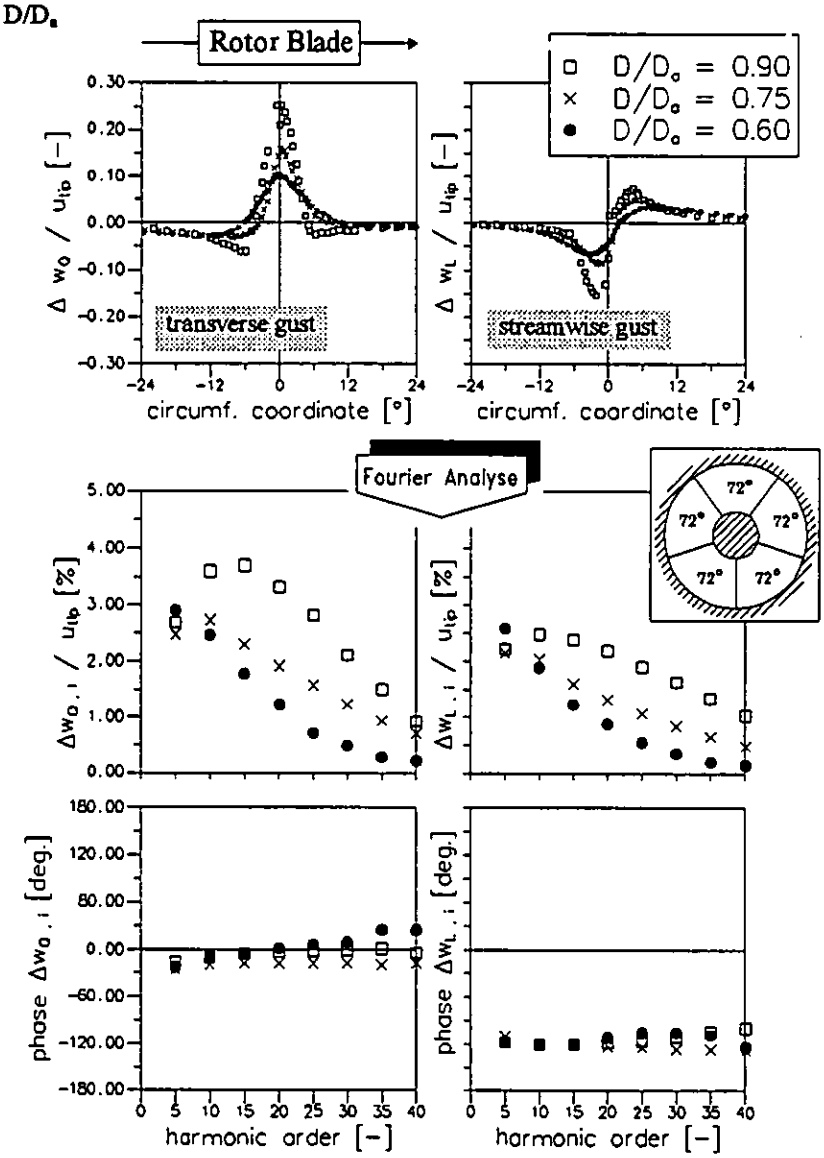

Figure 8 Gust velocities at rotor inlet due to wakes of struts

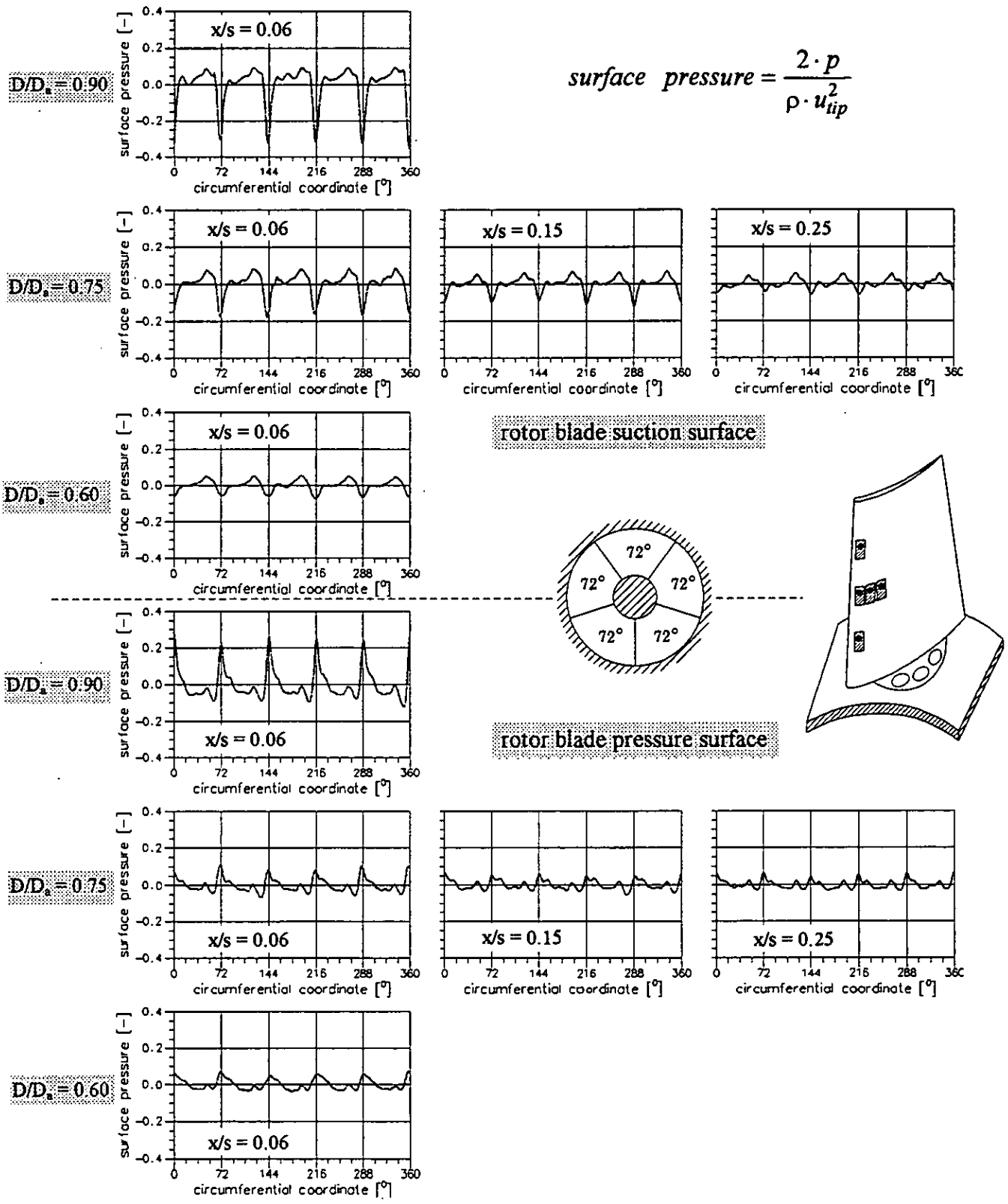

Figure 9 Rotor blade surface pressure response

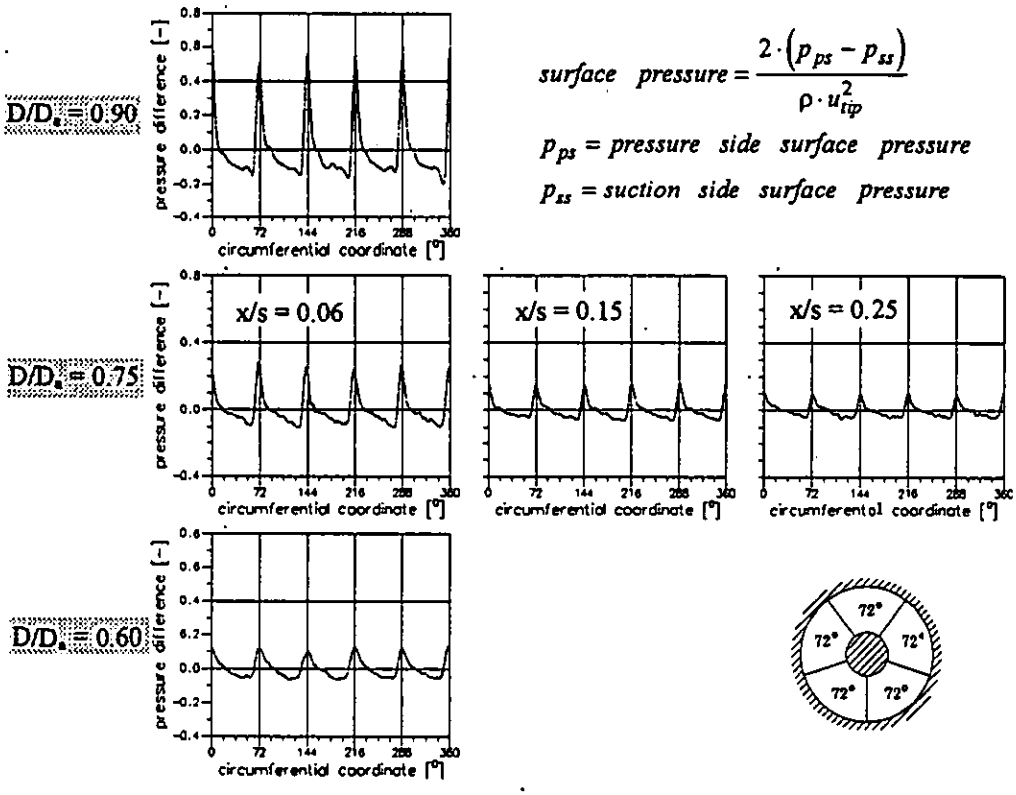

$$surface\ \ pressure = \frac{2 \cdot \left(p_{ps} - p_{ss}\right)}{\rho \cdot u_{tip}^2}$$

p_{ps} = *pressure side surface pressure*

p_{ss} = *suction side surface pressure*

Figure 10 Rotor blade surface pressure difference response

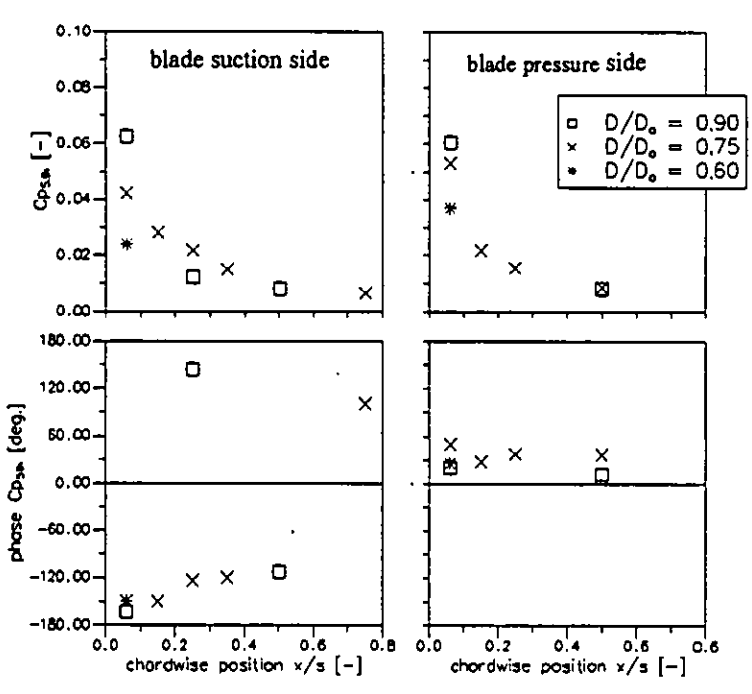

Figure 12 Fundamental surface pressure response amplitude (5th e.o.) due to strut wakes the at rotor inlet (Fig. 1)

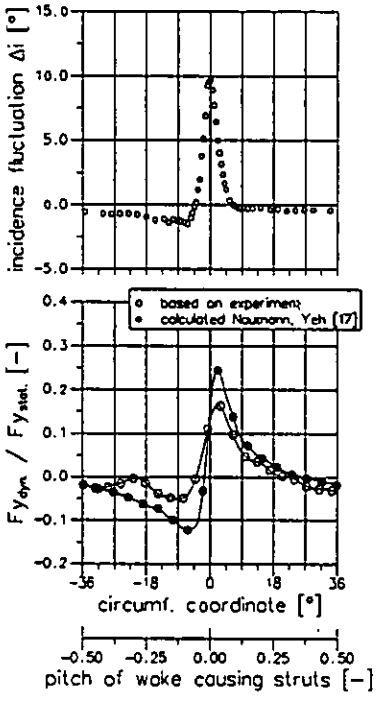

Figure 13 Unsteady rotor blade normal force (at midspan)

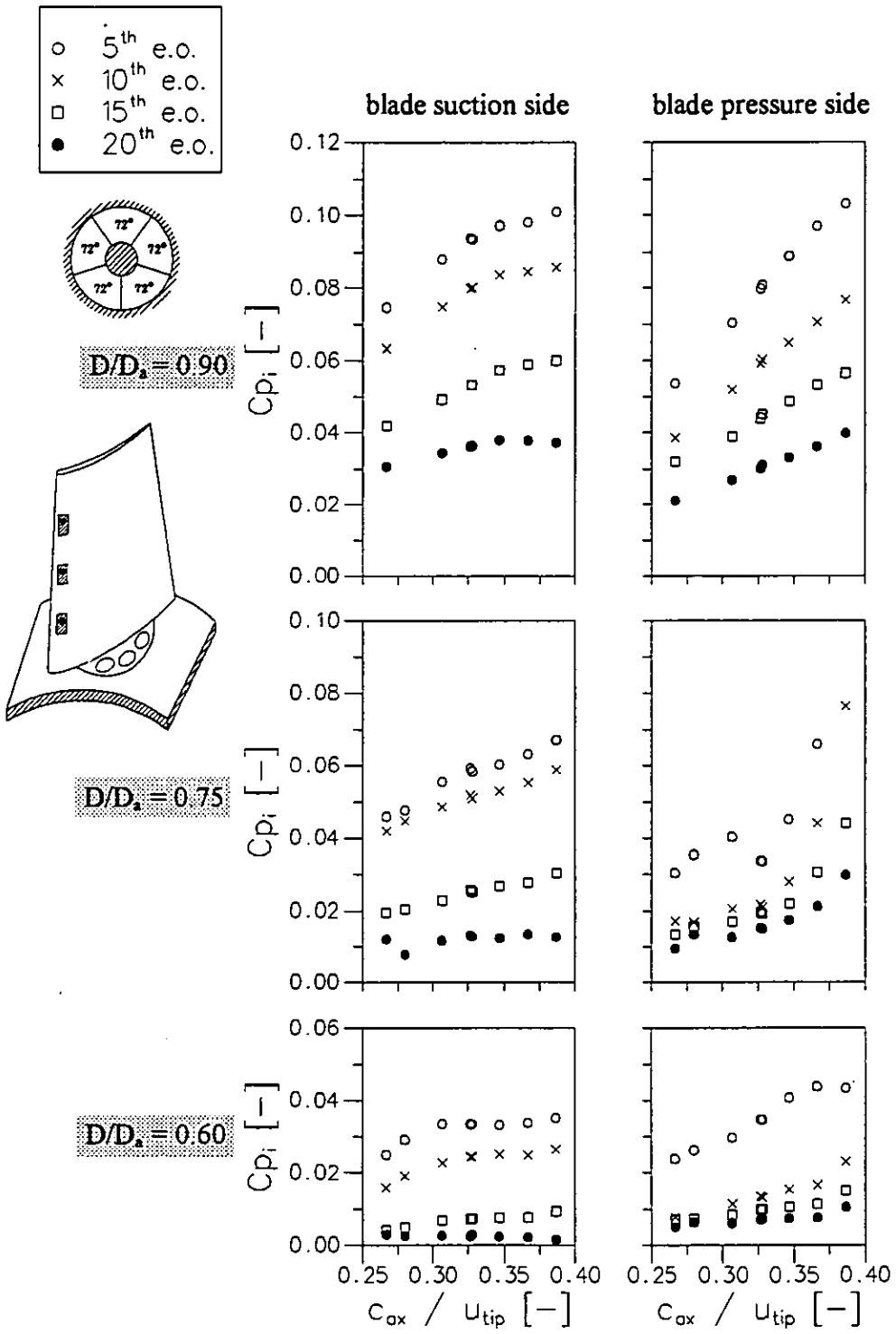

Figure 11 Harmonic surface pressure response amplitudes recorded near rotor blade leading edge (x/s = 0.06) vs. fan stage loading